Harrison L. Bartlett[1]
Mechanical Engineering,
Vanderbilt University,
Nashville, TN 37235
e-mail: harrison.l.bartlett@vanderbilt.edu

Brian E. Lawson
Mem. ASME
Mechanical Engineering,
Vanderbilt University,
Nashville, TN 37235
e-mail: brian.e.lawson@vanderbilt.edu

Michael Goldfarb
Professor
Fellow ASME
Mechanical Engineering,
Vanderbilt University,
Nashville, TN 37235
e-mail: michael.goldfarb@vanderbilt.edu

Optimal Transmission Ratio Selection for Electric Motor Driven Actuators With Known Output Torque and Motion Trajectories

This paper presents a method for selecting the optimal transmission ratio for an electric motor for applications for which the desired torque and motion at the transmission output are known a priori. Representative applications for which the desired output torque and motion are periodic and known include robotic manipulation, robotic locomotion, powered prostheses, and exoskeletons. Optimal transmission ratios are presented in two senses: one that minimizes the root-mean-square (RMS) electrical current and one that minimizes the RMS electrical power. An example application is presented in order to demonstrate the method for optimal transmission ratio selection.
[DOI: 10.1115/1.4036538]

1 Introduction

For a given motor, a common method for the selection of a transmission ratio is to employ a "quasi-static" approach that scales the continuous or short-term torque and/or speed operating characteristics of the motor to the continuous or short-term torque and/or speed operating requirements at the output. This approach essentially uses the transmission ratio to map the rated performance limits of the motor to those of the application. Since this type of approach does not consider motor dynamics, however, it may in the presence of significant dynamic effects in the motor provide a suboptimal, and in some cases, inappropriate determination of the transmission ratio [1].

In order to provide a more optimal selection of motor and/or transmission ratio, a number of researchers have presented various methods of motor and/or transmission selection that accounts for the passive dynamic elements present in the motor, transmission, and/or load. In Ref. [2], the authors describe a means of selecting an optimal transmission ratio for a motor, assuming a point-to-point motion and a purely inertial load. In Refs. [1] and [3], the authors present a method for motor selection for an a priori known torque-speed trajectory (i.e., for a generic load). The essential method of Refs. [1] and [3] was further refined and extended in Refs. [4–13]. The work in this field has primarily focused on motor selection [12,14,15], setting feasible bounds on transmission ratio selection [1,6–9], and the optimal selection of the transmission ratio [2,4,5,10,12,13].

The work presented in this paper is a further extension and refinement of Refs. [1] and [3] and the associated extensions of it. This work specifically extends these aforementioned prior works by: (1) providing optimal solutions in terms of minimizing root-mean-squared (RMS) current and RMS electrical power, respectively; (2) presenting these respective optimal solutions as closed-form analytical solutions (where possible); and (3) presenting the feasible limits of the motor in the context of rated electrical characteristics. This paper also leverages a bond graph formulation to represent the energetic structure of the motor–transmission–load interaction, which the authors employ to diagram the derivation of the transmission optimization expressions. The bond graph formulation is employed to derive new findings regarding the minimization of electrical power consumption and the feasible limitations of transmission ratio choice. The utility of the presented methodology lies in the simplicity of the models presented. The method is intended to be used by designers to quickly size electromechanical actuator components and to quantify the tradeoffs associated with different design decisions.

2 Methods

The components of an actuator for an electromechanical system, consisting of a motor and transmission driving a load, can be schematically represented as shown in Fig. 1. In this model, the motor has a torque constant K_τ, rotor inertia J, and electrical terminal resistance R; the transmission has a ratio of N:1 and mechanical efficiency η; and the load is described by a desired

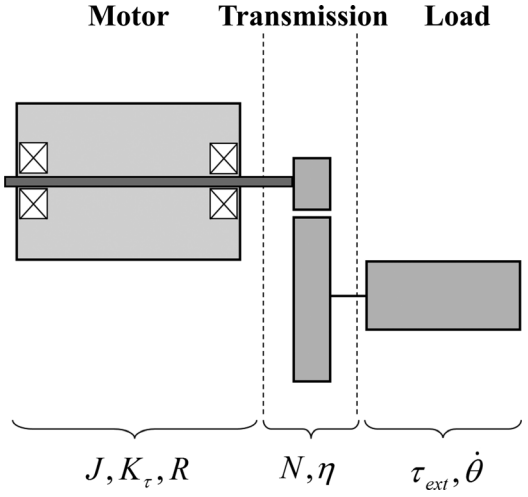

Fig. 1 The electromechanical actuator model treated here is split into three components: the motor, transmission, and load, each with associated constants and parameters

[1]Corresponding author.

Contributed by the Dynamic Systems Division of ASME for publication in the Journal of Dynamic Systems, Measurement, and Control. Manuscript received July 12, 2016; final manuscript received March 9, 2017; published online June 28, 2017. Assoc. Editor: Ardalan Vahidi.

angular velocity and torque trajectory defined by $\dot{\boldsymbol{\theta}}$ and $\boldsymbol{\tau}_{\text{ext}}$. It should be noted that the transmission efficiency, η, is assumed to be constant across different values of the transmission ratio, N, as well as across different values of $\dot{\boldsymbol{\theta}}$ and $\boldsymbol{\tau}_{\text{ext}}$. This assumption is reasonable for certain types of transmissions such as belts and chains, but is less reasonable for other transmission types [16]. However, the intention of this methodology is to remain agnostic with respect to transmission type. Should a designer have already decided upon a specific mechanism for the transmission, the model could be updated with the appropriate dynamic elements associated with that mechanism.

2.1 Minimizing Motor Torque. For a given motor and desired output angle and torque trajectories (i.e., output kinematics and kinetics), a transmission ratio can be selected to minimize the RMS motor torque, which will in turn minimize the RMS current into the motor and thus will minimize the Joule heating in the motor windings. A bond graph approach, as first described by Paynter [17] and Karnopp et al. [18], provides a useful power-domain-independent framework for formulation of the optimization problem. A bond graph of a motor coupled with a transmission is shown in Fig. 2(*a*). In this model, the effort and flow associated with the input are given by τ_m and $\dot{\theta}_m$ (motor torque and angular velocity), respectively. The model additionally incorporates passive inertia and damping behaviors, both associated with the motor flow variable. Additionally, the transmission is modeled as a linear transformer with transmission ratio N, and the effort and flow associated with the (mechanical) load are given by τ_{ext} and $\dot{\theta}$, respectively. The power loss associated with transmission inefficiency is modeled as a modulated resistance where η is the mechanical efficiency of the transmission. Reflecting the dynamical behavior of the actuator across the transmission and into the load domain yields the bond graph shown in Fig. 2(*b*), where the motor impedance consists of the combination of rotational inertia and damping, described by the linear coefficients J and b. It should be noted that causality is not assigned in this model because the results derived from the system are independent of such assignment.

In this model, τ_{ext} and $\dot{\theta}$ are known over time and defined by the desired kinematic and kinetic trajectory at the system output. Effort continuity around the one-junction in Fig. 2(*b*) yields

$$N\tau_m = JN^2\ddot{\theta} + bN^2\dot{\theta} + \tau_{\text{ext}} + \tau_{\text{ext}}\left(\eta^{-\text{sgn}(\tau_{\text{ext}}\dot{\theta})} - 1\right) \tag{1}$$

Since all the bonds are connected to the same common flow junction, expression (1) becomes a power balance by multiplying both sides of the expression by the common flow ($\dot{\theta}$). The first two terms in the right-hand side of Eq. (1) represent the output torque lost to the internal impedance of the actuator. Factoring N^2 out of these two terms yields a simplifying variable, β, given by

$$\beta = J\ddot{\theta} + b\dot{\theta} \tag{2}$$

The third term on the right-hand side of Eq. (1) represents the torque delivered to the load of the actuator, while the fourth term represents the torque required to overcome transmission inefficiencies. The transmission efficiency is dependent on the net direction of power flow, giving rise to the nonlinear nature of this fourth term. It should be noted that in this model, positive power is defined as power flowing from the motor to the load. In an effort to simplify subsequent expressions, an asymmetric efficiency-based multiplier (ε) is utilized to capture the effects of transmission efficiency

$$\varepsilon = \eta^{-\text{sgn}(\tau_{\text{ext}}\dot{\theta})} \tag{3}$$

Utilizing the simplifying terms given in Eqs. (2) and (3), Eq. (1) reduces to the more compact expression

$$N\tau_m = \beta N^2 + \varepsilon\tau_{\text{ext}} \tag{4}$$

From Eq. (4), an explicit expression for the input effort (motor torque) can be derived

$$\tau_m = \beta N + \frac{\tau_{\text{ext}}}{N}\varepsilon \tag{5}$$

and the transmission ratio $N = N^*_{\tau_m}$ that minimizes this effort can be found from Eq. (5) as

$$N^*_{\tau_m} = \sqrt{\frac{\varepsilon\tau_{\text{ext}}}{\beta}} \tag{6}$$

In the case of an electric motor driven transmission, motor impedance is typically dominated by rotor inertia ($\beta = J\ddot{\theta}$). Additionally, because motor torque τ_m is proportional to applied current i, the transmission ratio N that minimizes motor torque (6) will also minimize motor current. The solution described by Eq. (6), however, is limited to a single instance of torque and angular acceleration, due to the scalar nature of its inputs.

The analysis presented earlier can be extended to optimize N with respect to a complete desired drive system trajectory defined by $\boldsymbol{\tau}_{\text{ext}}$ and $\ddot{\boldsymbol{\theta}}$, where the vector notation indicates that each variable describes the respective time history over the course of the actuator's actuation cycle. In the vector case, the current consumed by the motor for this desired trajectory can be derived by substituting $\boldsymbol{\beta} = J\ddot{\boldsymbol{\theta}}$ and $\boldsymbol{\tau}_m = K_\tau\ \mathbf{i}$ into Eq. (5) and isolating $\mathbf{i}$

$$\mathbf{i} = \frac{\boldsymbol{\tau}_{\text{ext}}\boldsymbol{\varepsilon} + J\ddot{\boldsymbol{\theta}}N^2}{K_\tau N} \tag{7}$$

Note that vector multiplication, as used herein, is intended to represent elementwise multiplication. The RMS of this current trajectory can be minimized by choosing the appropriate transmission ratio

$$\text{RMS}(\mathbf{i}) = \text{RMS}\left(\frac{\boldsymbol{\tau}_{\text{ext}}\boldsymbol{\varepsilon} + J\ddot{\boldsymbol{\theta}}N^2}{K_\tau N}\right) \tag{8}$$

The transmission ratio N that minimizes Eq. (8), the derivation of which can be found in the Appendix, is given by

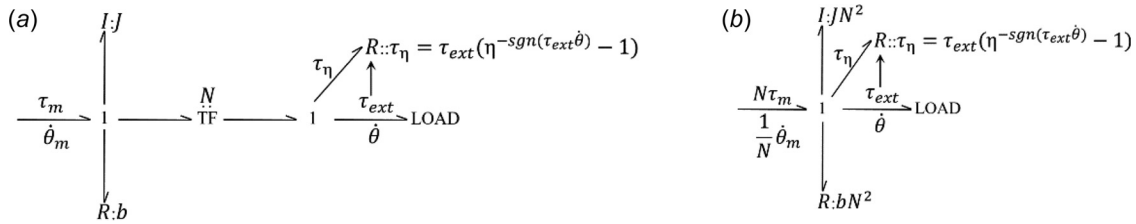

Fig. 2 (*a*) The bond graph of a mechanical transmission with state-dependent impedances associated with its power source and known output efforts and flows and (*b*) the same system reflected into the output domain

$$N^*_{\mathrm{RMS(i)}} = \sqrt{\frac{\mathrm{RMS}(\tau_{\mathrm{ext}}\boldsymbol{\varepsilon})}{\mathrm{RMS}(J\ddot{\boldsymbol{\theta}})}} \tag{9}$$

It should be noted that Eq. (9) is a general expression that encapsulates Eq. (6). Additionally, for a purely inertial load ($\tau_{\mathrm{ext}} = J\ddot{\boldsymbol{\theta}}$), Eq. (9) reduces to the optimal transmission ratio found previously by Pasch and Seering [2]. Similar findings were also presented in Refs. [5], [11], and [12]. However, the asymmetric efficiency term is additionally included here in the expression for the optimal transmission ratio. The model presented here also allows for the inclusion of additional impedance terms in the motor such as bearing friction. The dynamic effects considered in this work can be easily altered or extended by changing either the τ_{ext} or β term.

2.2 Minimizing Actuator Power Consumption. Electromechanical drive systems may also be concerned with electrical power consumption. As such, a transmission ratio can alternatively be selected such that the electrical energy consumed by the actuator over a cycle is minimized. Figure 3 shows a bond graph model similar to that shown in Fig. 2(*a*), but with the electrical domain of the motor included as well. Specifically, the model includes a terminal resistance R, an applied voltage V_{in}, a voltage across the resistor V_R, a current i, and a back electromotive force (EMF) voltage V_{emf}. The motor is also assumed here to have negligible electrical inductance ($L \approx 0$), although a non-negligible inductance could be included if needed. From this bond graph model, the below relations follow:

$$V_{\mathrm{in}} = iR + K_\tau N\dot{\theta} \tag{10}$$

$$i = \frac{\tau_{\mathrm{ext}}\varepsilon + \beta N^2}{K_\tau N} \tag{11}$$

The product of Eqs. (10) and (11) provides an expression for the power into the actuator

$$P_{\mathrm{in}} = V_{\mathrm{in}} i = \frac{\beta N + \frac{\tau_{\mathrm{ext}}}{N}\varepsilon}{K_\tau}\left[\frac{R}{K_\tau}\left(\beta N + \frac{\tau_{\mathrm{ext}}}{N}\varepsilon\right) + K_\tau N\dot{\theta}\right] \tag{12}$$

which can be used to find the transmission ratio N that minimizes the input power to the motor

$$N^*_{P_{\mathrm{in}}} = \sqrt[4]{\frac{(\tau_{\mathrm{ext}}\varepsilon)^2}{\beta^2 + \left[\frac{K_\tau^2\beta\dot{\theta}}{R}\right]}} = \sqrt[4]{\frac{(\tau_{\mathrm{ext}}\varepsilon)^2}{\beta^2 + \mathrm{K_m^2}\beta\dot{\theta}}} \tag{13}$$

where $K_m = (K_\tau/\sqrt{R})$, which is sometimes referred to as the motor constant or the speed torque gradient [15,19,20].

Solving for an analytical expression for the transmission ratio that minimizes RMS motor power consumption is not tractable because it produces an eighth-order polynomial. However, the minima can be found numerically using

$$N^*_{\mathbf{P}_{\mathrm{in}}} = \underset{N}{\mathrm{argmin}}\left[\mathrm{RMS}\left(\frac{J\ddot{\boldsymbol{\theta}}N + \frac{\boldsymbol{\tau}_{\mathrm{ext}}}{N}\boldsymbol{\varepsilon}}{K_\tau}\left[\frac{R}{K_\tau}\left(J\ddot{\boldsymbol{\theta}}N + \frac{\boldsymbol{\tau}_{\mathrm{ext}}}{N}\boldsymbol{\varepsilon}\right) + K_\tau N\dot{\boldsymbol{\theta}}\right]\right)\right] \tag{14}$$

In Eq. (14), it is again assumed that the motor impedance is dominated by the rotor inertia ($\boldsymbol{\beta} = J\ddot{\boldsymbol{\theta}}$).

2.3 Applying Practical Limits to Transmission Ratios. The solution set of transmission ratios is bounded by the torque, speed, and thermal limitations of a motor, and the optimal transmission ratio(s) previously expressed may not lie within the bounded solution set.

2.3.1 Saturation Limits. The current available to a motor ($\hat{\mathbf{i}}$) during a given actuator output angular velocity trajectory ($\hat{\boldsymbol{\theta}}$) is given by

$$\hat{\mathbf{i}} = \frac{V}{R} - \frac{K_\tau N|\dot{\boldsymbol{\theta}}|}{R} \tag{15}$$

where V is the electrical supply rail voltage. In order for the actuator to satisfy a desired torque trajectory, the current available to the motor must be greater than or equal to the current required by the motor ($\hat{\mathbf{i}} \geq |\hat{\mathbf{i}}|$), which can be expressed by

$$\frac{V}{R} - \frac{K_\tau N|\dot{\boldsymbol{\theta}}|}{R} - \left|\frac{J\ddot{\boldsymbol{\theta}}N}{K_\tau} + \frac{\boldsymbol{\tau}_{\mathrm{ext}}\boldsymbol{\varepsilon}}{K_\tau N}\right| \geq 0 \tag{16}$$

Every entry in the vector described by Eq. (16) must be greater than or equal to zero in order for the actuator to successfully perform the task. The first term in Eq. (16) represents the nominal current through the motor, while the second term describes the effective current lost to back EMF. The third and fourth terms in Eq. (16) describe the current required by the desired trajectory both to overcome the motor's internal impedance and to deliver torque to the load. The range of N for which Eq. (16) is satisfied can be easily found numerically by evaluating Eq. (16) at different values of N.

The lower bound of this range describes a torque limitation of the motor, while the upper bound describes an angular velocity limitation of the motor. If no value of N satisfies Eq. (16), then the motor cannot perform the desired task with the supply voltage used. A larger supply voltage (V) increases the solution range of transmission ratios, however, the motor still may encounter thermal limitations.

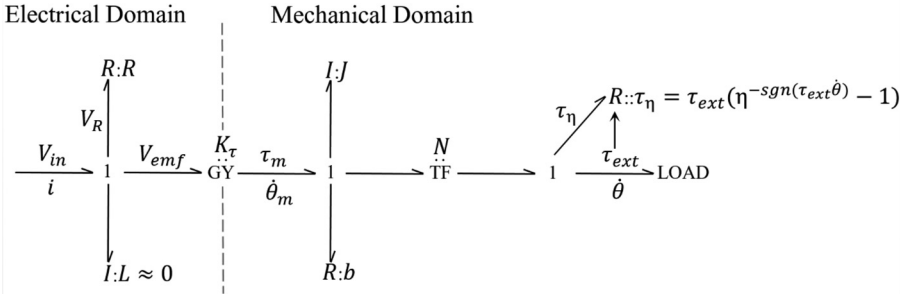

Fig. 3 The bond graph of a direct current motor and a mechanical transmission driving a load with desired kinematics and kinetics. The motor electrical inductance is assumed to be negligible.

2.3.2 Thermal Limits. In addition to the saturation limitations on the transmission ratio solution range imposed by the stall torque and no load speed of the motor, the motor is also limited by its thermal dynamics. The RMS of the current trajectory must remain below the maximum continuous current capacity of the motor (i_{cont}). At low transmission ratios, a large current is required to achieve a given maximum output torque. At high transmission ratios, a large current is required to overcome the torques required to produce passive dynamics of the motor to achieve a given output velocity (i.e., in the case of motor damping) and/or acceleration (i.e., in the case of motor inertia). It is the tradeoff between these two effects that produces the minimization described previously. A lower and upper thermal bound for the transmission ratio (N_{T_L} and N_{T_U}) will be defined as the upper and lower transmission ratios for which the following expression is satisfied:

$$\text{RMS}(\mathbf{i}) = i_{\text{cont}} \tag{17}$$

It should be noted that Eq. (17), while providing a useful reference regarding the thermal limitations of a motor, provides only a necessary condition on the maximum allowable amount of RMS motor current, not a sufficient one. A motor with RMS current above i_{cont} will exceed the thermal limits of the motor, but a motor with RMS current below i_{cont} will not necessarily operate within the thermal limits. Short-term peaks in current acting through the thermal dynamics of a motor could be sufficient to exceed allowable winding temperatures. As such, although Eq. (17) provides a useful reference, the requisite motor current for a given transmission ratio could also be checked against a thermal model of the motor to ensure that both necessary and sufficient conditions are satisfied [21].

2.3.3 Existence of a Transmission Ratio Solution. The solution set of transmission ratios can be bracketed between the ranges specified by both the thermal limitations and the torque/speed saturation limitations of the motor (range in which the motor can accomplish the task successfully without encountering saturation or thermal limitations). A lower bound for the transmission ratio N_L is the minimum value of N in this range, while N_U is the upper bound and largest value of N for this range. The upper and lower bounds are defined by the most restrictive set of transmission ratios for which the motor does not saturate or exceed its thermal limits. It should be noted that if no such range exists, then the motor cannot provide the desired torque and motion trajectories for any transmission ratio.

3 Design Application

As an example application of the method presented above, consider the design of an electromechanical drive system for the swing phase of a one degree-of-freedom transtibial prosthesis. In this example, a passive mechanism is assumed to provide ankle torque during the stance phase of walking, while an actuated system is used to provide dorsiflexion of the prosthesis during swing phase. In this drive system, the power associated with the powered push off phase of gait is not supplied by the drive system, allowing a low-powered motor to be utilized. The actuator for this system must be compact and deliver the desired kinematics and kinetics for the application. To determine the actuator design for this system, the kinematics and kinetics of the joint must be determined, candidate motors must be selected, and the transmission optimization must be applied to each candidate motor.

The necessary actuator kinematics and torque for this application can be seen in Fig. 4. It should be noted that viscous damping dominates the system dynamics, and because of this, the optimum transmission ratio described in Ref. [2] will not provide an accurate solution for this application. The product of the joint angular velocity and torque yields a curve with qualitatively the same shape as the torque curve shown in Fig. 4(*d*) with a peak joint power over the cycle of 9.5 W.

3.1 Candidate Motor Selection. Based on the peak joint power requirement of 9.5 W, two candidate motors were selected for the application: a Maxon EC 16 8 W motor and a Maxon EC 45 12 W motor. A brief overview of the relevant motor specifications for both candidate motors is given in Table 1. In this design example, the supply voltage was set at 48 V.

3.2 Transmission Optimization. For each of the two candidate motors and the desired kinematic and kinetic output trajectories shown in Fig. 4, the RMS current and RMS power of the motor were calculated for a wide range of transmission ratios using the previously described method. In this analysis, transmission mechanical efficiency was assumed to be 80% ($\eta = 0.8$). Additionally, the transmission ratios that minimize each of these

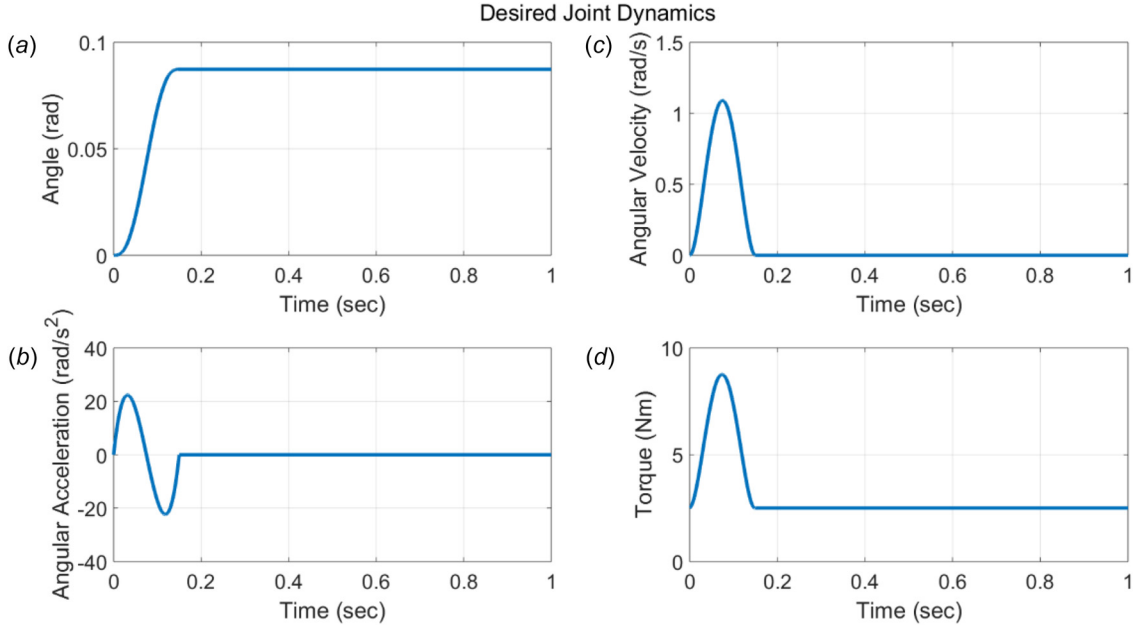

Fig. 4 Desired output dynamics of robotic ankle prosthesis actuator for dorsiflexion of the ankle during level ground walking: (*a*) ankle angle, (*b*) ankle angular velocity, (*c*) ankle angular acceleration, and (*d*) ankle torque

Table 1 Motor specifications

	EC 16	EC 45
Nominal power (W)	8	12
Rotor inertia, J (g cm^2)	0.85	52.3
Torque constant, K_τ (mN m/A)	18.7	30.5
Supply voltage, V (V)	48	48
Max continuous current, i_{cont} (A)	0.461	0.766
Terminal resistance, R (Ω)	20.5	6.42

two quantities were calculated using Eqs. (9), (10), and (14). Transmission bounds were also calculated using Eqs. (16) and (17). A plot of these curves, their minima, and the feasible transmission bounds are shown in Fig. 5. The thermal limits, given by Eq. (17), are plotted as dark gray vertical dashed lines, while the torque and speed saturation limits given by Eq. (16) are plotted as light gray vertical dashed lines. It should be noted that the upper thermal and saturation bounds are off the right end of the plot for the EC 16 motor in Fig. 5. The double y-axis plot allows for all of the relevant curves and points to be plotted on a single plot for each motor and transmission combination generating the desired output trajectories. The RMS motor current is plotted against the left y-axis, while the RMS motor power is plotted against the right y-axis. The maximum continuous current, as given by the motor data sheets, is also plotted as a dashed horizontal line to give reference for the current curves with respect to the limitations of the motor. Transmission selection should be performed by attempting to minimize the motor current and/or power associated with performing the desired activity (minimums of the curves in Fig. 5) subject to the feasible limitations imposed by saturation and thermal limits of the motor and electrical supply (vertical lines in Fig. 5).

From Fig. 5, a motor and transmission pairing can be made with knowledge of that pairing's effect on important system performance parameters. The RMS current of the motor should be minimized to minimize Joule heating of the motor, while the RMS power curve should be minimized for the longevity of a battery-powered device. Additionally, the flatness of the curves can be examined in the regions of interest to see if small changes in transmission ratio have large effects on the performance metric curves (RMS($\mathbf{i}$) and RMS($\mathbf{P}_{in}$) as a function of N). By examining the shapes of these curves, small transmission ratios can be chosen while still approaching the minima of the performance metric curves.

The difference in the shapes of the curves in Fig. 5 for the two motors can be largely attributed to the motors' construction. The EC 16 motor is an internal rotor brushless motor, while the EC 45 is an external rotor flat brushless motor. The difference in construction is reflected in the differences in the two motors' rotor inertias and torque constants (Table 1). The high torque density of external rotor motors allows for small transmission ratios, but at the cost of high rotor inertias [22,23]. These high rotor inertias become significant to the system dynamics at high transmission ratios due to reflected inertia. The effects of the large rotor inertia can be seen in Fig. 5(*b*) in which the performance metric curve minima is much more pronounced than the internal rotor counterpart shown in Fig. 5(*a*). At high values of N, the reflected inertia becomes very large and the motor consumes large amounts of current in order to accelerate and decelerate the rotor inertia.

For this application, the EC 45 motor would be paired with a transmission ratio of approximately 250:1 in order to minimize both the maximum motor current and RMS motor power. The EC 16 motor would be paired with a transmission ratio of approximately 600:1 in order to stay within the transmission bounds while maintaining a minimal transmission and minimize power consumption. The plots shown in Fig. 5 help to illustrate tradeoffs in the actuator design. The shapes of the curves, the feasible transmission ratio ranges, as well as the minimums can aid in the actuator design process. The tradeoffs illustrated by this method must be balanced with other design constraints such as size or mass limits or other characteristics of the actuator.

4 Discussion

As demonstrated by the previous example, consideration of the dynamics of a motor is important in the choice of motor and transmission ratio, particularly for applications involving substantial variation in motion. By including the dynamic characteristics of a motor in a systematic process for selecting a transmission ratio, higher performance actuation systems can be designed. The method of actuator design and transmission ratio selection presented here provides a quantitative method for examining the tradeoffs between different transmission ratio choices on relevant system performance characteristics. Specifically, the tradeoffs

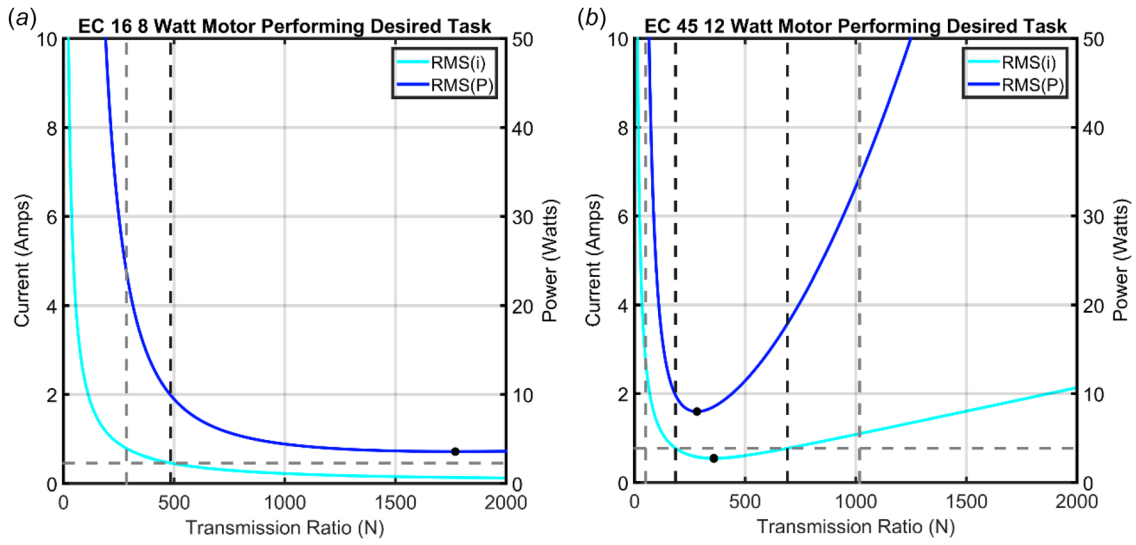

Fig. 5 Actuator RMS current, peak current, and RMS power plotted against transmission ratio with feasible transmission bounds marked by vertical dashed lines. Dark-dashed lines indicate thermal bounds, gray vertical dashed lines indicate a torque or speed limitation, and the horizontal dashed lines are the motor's specified maximum continuous current. Current values are plotted against the left *y*-axis, while power values are plotted against the right *y*-axis. Two motors executing the same task are plotted in this figure: (*a*) EC 16 8 W (The upper thermal bound is off the right end of the plot) and (*b*) EC 45 12 W.

between motor current consumption and power consumption are considered. In this regard, the curves as shown in Fig. 5 may be of more use to designers than the specific optima described in this paper. From this standpoint, a designer can balance the performance characteristics that are most relevant or critical for a given application. Similarly, different motors performing the same desired task can be quantitatively compared. The relative size, power consumption, and electrical requirements of different candidate actuators can be quickly examined in this way.

As can be seen from Eq. (16), increasing the supply voltage to the motor can increase the size of the solution set of transmission ratios for the motor. However, there is a limit to how much the supply voltage can be increased. At some point, torque and speed saturation will no longer be the limiting factor constraining the range of transmission ratios for the actuator, and instead the thermal limitations of the motor will be the most constraining factor. A supply voltage and transmission ratio may be chosen simultaneously using this method so that the smallest electrical supply that still allows for successful actuator performance is chosen. This insight may enable one to more appropriately size the electrical supply voltage for a given actuator.

This simple model-based method provides a procedure by which transmission ratio, N, can be chosen, although the physical implementation of the transmission (gearhead, cable drive, etc.) must be determined by the designer. The inclusion of transmission efficiency in this model also allows designers to examine the effects of using different transmission types with different efficiencies for the same application.

The previously mentioned method presented by Pasch [2] is intended for purely inertial loads, while the method presented in this paper can accommodate an arbitrary desired output kinematic and kinetic trajectory. For systems in which the inertial torques dominate the system kinetics, the method presented in this paper will yield similar optimal solutions to the Pasch and Seering method, and for systems with purely inertial loads ($\tau_{\text{ext}} = I\ddot{\theta}$), the two methods will yield identical solutions.

One limitation of this method is that it assumes that transmission efficiency is constant across different values of the transmission ratio. To accommodate for this limitation, an explicit expression for transmission efficiency as a function of transmission ratio, torque, and velocity could be substituted into the equations described previously and the new minima could be found either analytically or numerically. Another limitation to the method is that it does not include the inertia of the transmission itself. However, if the transmission inertia is significant, the torque required to accelerate and decelerate the transmission inertia can be included in the desired kinetic trajectory, thereby accounting for this impedance. It should also be pointed out that this method assumes that power can flow both into and out of the actuator. Because of this, there is an implicit assumption that the actuator is being controlled by a servo amplifier capable of regeneration.

The treatment of motor dynamics in the selection of transmission ratio also illuminates the fact that high transmission ratios are not always more beneficial for achieving a desired torque trajectory. As can be seen in Fig. 5(*b*), high transmission ratios decrease system performance due to the effects of the reflected rotor inertia. Even in cases of small motor inertia, there is a plateau beyond which larger transmission ratios produce only small gains in current and power minimization. In fact, for any motor performing any application, the motor current and power will approach infinity at both very small and very large transmission ratios, suggesting an optimum value of N will always assume an intermediate value between these two extremes.

5 Conclusions

The authors have presented here an extension of prior literature focused on the optimal selection of a transmission ratio. In particular, this work considers the influence of passive electrical and mechanical properties of the motor on transmission selection for a general load and extends prior work on the subject by: (1) providing optimal solutions in terms of electrical power, specifically in the sense of minimizing RMS current and RMS electrical power, respectively; (2) presenting these respective optimal solutions in closed-form analytical manner (where possible); and (3) presenting the feasible limits of the motor in the context of rated electrical characteristics. In addition to providing a quantitative solution, the method makes clear that in general, an optimal transmission ratio will exist between a lower bound associated with meeting steady-state output torque requirements, and an upper bound associated with dynamic effects in the motor, which are exacerbated at higher transmission ratios.

Funding

This material is based upon the work supported by the National Science Foundation Graduate Research Fellowship Program under Grant No. 1445197.

Nomenclature

b = generalized viscous damping
i = motor current
I = load inertia
i_{cont} = maximum continuous motor current
J = motor rotor inertia
K_τ = motor torque constant
L = motor inductance
N = transmission ratio
N_T = transmission ratio bound due to thermal limit
N_j^* = optimal transmission ratio with respect to j
P_{in} = power into actuator
R = motor terminal resistance
V = electrical supply rail voltage
V_R = voltage across motor windings
V_{EMF} = back EMF voltage
V_{in} = voltage applied to motor
β = motor impedance term
ε = asymmetric efficiency term
η = transmission mechanical efficiency
θ = actuator output position
θ_m = motor position
τ_m = motor torque
τ_{ext} = actuator output torque

Appendix: Derivation of Root-Mean-Square Minima

It should be noted that all the vector operations mentioned above are elementwise multiplication, but vector operations in this section obey standard vector operations and "$\circ$" indicates elementwise multiplication.

To minimize Eq. (8), an explicit expression of RMS(**i**) can be written as

$$\text{RMS}(\mathbf{i}) = \sqrt{\frac{\mathbf{i}\mathbf{i}^{\text{T}}}{\text{size}(\mathbf{i})}} \tag{A1}$$

In order to minimize Eq. (A1) and subsequently Eq. (8), the numerator inside the radical in Eq. (A1) should be minimized. This minimization is done by taking the derivative of this numerator with respect to N, setting that expression equal to zero and solving for N

$$\frac{\partial \mathbf{i}\mathbf{i}^{\text{T}}}{\partial N} = 2\mathbf{i}\left(\frac{\partial \mathbf{i}}{\partial N}\right)^{\text{T}} = 0 \tag{A2}$$

Substituting Eq. (7) for **i** in Eq. (A2), the following expression can be derived:

$$\frac{2}{K_\tau}\left(\frac{\boldsymbol{\varepsilon}\circ\boldsymbol{\tau}_{\text{ext}}}{N}+J\ddot{\boldsymbol{\theta}}N\right)\left(\frac{-(\boldsymbol{\varepsilon}\circ\boldsymbol{\tau}_{\text{ext}})^{\text{T}}}{N^2}+J\ddot{\boldsymbol{\theta}}^{\text{T}}\right)=0 \tag{A3}$$

The expression in Eq. (A3) can then be simplified to an expression in which each term is a scalar

$$\frac{2}{K_\tau}\left(\frac{-(\boldsymbol{\varepsilon}\circ\boldsymbol{\tau}_{\text{ext}})(\boldsymbol{\varepsilon}\circ\boldsymbol{\tau}_{\text{ext}})^{\text{T}}}{N^3}+J^2N\ddot{\boldsymbol{\theta}}\ddot{\boldsymbol{\theta}}^{\text{T}}\right)=0 \tag{A4}$$

and subsequently solved for N

$$N=\sqrt[4]{\frac{(\boldsymbol{\varepsilon}\circ\boldsymbol{\tau}_{\text{ext}})(\boldsymbol{\varepsilon}\circ\boldsymbol{\tau}_{\text{ext}})^{\text{T}}}{J^2\ddot{\boldsymbol{\theta}}\ddot{\boldsymbol{\theta}}^{\text{T}}}} \tag{A5}$$

This expression for N can then be simplified to match the expression seen in the primary text in the below equation

$$N^*_{\text{RMS}(\mathbf{i})}=\sqrt{\frac{\text{RMS}(\boldsymbol{\varepsilon}\circ\boldsymbol{\tau}_{\text{ext}})}{\text{RMS}(J\ddot{\boldsymbol{\theta}})}} \tag{A6}$$

References

[1] Van de Straete, H. J., Degezelle, P., De Schutter, J., and Belmans, R. J. M., 1998, "Servo Motor Selection Criterion for Mechatronic Applications," IEEE/ASME Trans. Mechatronics, **3**(1), pp. 43–50.

[2] Pasch, K. A., 1984, "On Drive Systems for High Performance Machines and Design of an Air Motor/Particle Brake Actuator," M.S. thesis, Massachusetts Institute of Technology, Cambridge, MA.

[3] Van de Straete, H. J., De Schutter, J., and Belmans, R., 1999, "An Efficient Procedure for Checking Performance Limits in Servo Drive Selection and Optimization," IEEE/ASME Trans. Mechatronics, **4**(4), pp. 378–386.

[4] Roos, F., Johansson, H., and Wikander, J., 2006, "Optimal Selection of Motor and Gearhead in Mechatronic Applications," Mechatronics, **16**(1), pp. 63–72.

[5] Cusimano, G., 2007, "Optimization of the Choice of the System Electric Drive-Device—Transmission for Mechatronic Applications," Mech. Mach. Theory, **42**(1), pp. 48–65.

[6] Cusimano, G., 2011, "Choice of Electrical Motor and Transmission in Mechatronic Applications: The Torque Peak," Mech. Mach. Theory, **46**(9), pp. 1207–1235.

[7] Cusimano, G., 2013, "Influence of the Reducer Efficiencies on the Choice of Motor and Transmission: Torque Peak of the Motor," Mech. Mach. Theory, **67**, pp. 122–151.

[8] Cusimano, G., 2015, "Choice of Motor and Transmission in Mechatronic Applications: Non-Rectangular Dynamic Range of the Drive System," Mech. Mach. Theory, **85**, pp. 35–52.

[9] Choi, C., Jung, S., Kim, S., Lee, J., Choe, T., Chung, S., and Park, Y., 2007, "A Motor Selection Technique for Designing a Manipulator," International Conference on Control, Automation and Systems (ICCAS'07), Seoul, South Korea, Oct. 17–20, pp. 2487–2492.

[10] Pettersson, M., and Ölvander, J., 2009, "Drive Train Optimization for Industrial Robots," IEEE Trans. Rob., **25**(6), pp. 1419–1424.

[11] Rezazadeh, S., and Hurst, J. W., 2014, "On the Optimal Selection of Motors and Transmissions for Electromechanical and Robotic Systems," IEEE/RSJ International Conference on Intelligent Robots and Systems (IROS), Chicago, IL, Sept. 14–18, pp. 4605–4611.

[12] Giberti, H., Cinquemani, S., and Legnani, G., 2010, "Effects of Transmission Mechanical Characteristics on the Choice of a Motor-Reducer," Mechatronics, **20**(5), pp. 604–610.

[13] Giberti, H., Cinquemani, S., and Legnani, G., 2011, "A Practical Approach to the Selection of the Motor-Reducer Unit in Electric Drive Systems," Mech. Based Des. Struct. Mach., **39**(3), pp. 303–319.

[14] Giberti, H., Clerici, A., and Cinquemani, S., 2014, "Specific Accelerating Factor: One More Tool in Motor Sizing Projects," Mechatronics, **24**(7), pp. 898–905.

[15] Sensinger, J. W., 2010, "Selecting Motors for Robots Using Biomimetic Trajectories: Optimum Benchmarks, Windings, and Other Considerations," IEEE International Conference on Robotics and Automation (ICRA), Anchorage, AK, May 3–7, pp. 4175–4181.

[16] Shigley, J. E., and Mischke, C. R., 1986, *Standard Handbook of Machine Design*, McGraw-Hill, New York.

[17] Paynter, H. M., 1961, *Analysis and Design of Engineering Systems*, MIT Press, Cambridge, MA.

[18] Karnopp, D. C., Margolis, D. L., and Rosenberg, R. C., 1990, *System Dynamics: A Unified Approach*, Wiley, Hoboken, NJ.

[19] Braun, J., 2012, *Formulae Handbook*, Maxon Motors, Sachseln, Switzerland.

[20] Faulhaber, F., 2016, "Technical Information," Faulhaber, Schönaich, Germany.

[21] Paine, N., and Sentis, L., 2015, "Design and Comparative Analysis of a Retrofitted Liquid Cooling System for High-Power Actuators," Actuators, **4**(3), pp. 182–202.

[22] Reichert, T., Nussbaumer, T., and Kolar, J. W., 2009, "Torque Scaling Laws for Interior and Exterior Rotor Permanent Magnet Machines," IEEE International Magnetics Conference (INTERMAG 2009), Sacramento, CA, May 4–8, pp. 1–4.

[23] Sensinger, J. W., Clark, S. D., and Schorsch, J. F., 2011, "Exterior vs. Interior Rotors in Robotic Brushless Motors," IEEE International Conference on Robotics and Automation (ICRA), Shanghai, China, May 9–13, pp. 2764–2770.